Design and Implementation of a Multi-Parametric Geo-Seismic Realization Engine for Programmable Mechatronic IoT Geo-Mechanics Simulators

Hasan Tariq[1]
Department of Electrical Engineering
College of Engineering,
Qatar University
Doha, Qatar
hasan.tariq@qu.edu.qa

Abderrazak Abdaoui [1]
Department of Electrical Engineering
College of Engineering,
Qatar University
Doha, Qatar
abderrazak.abdaoui@qu.edu.qa

Farid Touati[1]
Department of Electrical Engineering
College of Engineering,
Qatar University
Doha, Qatar
touatif@qu.edu.qa

Mohammed Abdulla E Al-Hitmi[1]
Department of Electrical Engineering
College of Engineering,
Qatar University
Doha, Qatar
m.a.alhitmi@qu.edu.qa

Damiano Crescini[2]
Brescia University
Brescia, Italy
damiano.crescini@unibs.it

Adel Ben Manouer[3]
Canadian University Dubai
Dubai, UAE
adel@cud.ac.ae

***Abstract*—Physical simulation of seisms and earthquakes are a big challenge for disaster management agencies. Billions of dollars are spent annually to exercise seismic disaster preventive procedures. The current state of the art geo-seismic simulators use mechanical actuators like motors to perform ground motions, these motions need to be coherent with geo-seismic perception and ground mechanics. In this work, a programmable multi-parametric geo-seismic realization engine has been proposed to improve the capabilities of existing mechatronic ground simulators as 1:1 correspondence equivalent simulation. The seismic waves, wave patterns, wave velocities, wave amplitudes, wave pattern amplitudes, pattern frequencies, distances traveled, epicenters, hypo-centers, seismic centers, and arrival angles of incidence with respect to poles and equator, hypo-epi central distance, and ground/seismic station was modeled for motor based motion control system. The geo-seismic realization parameters and ground motions were equated dot by dot. The geo-seismic realization engine was tested for a wide range of ground motions with extreme seismic waves from 0.1Hz to 178Hz, velocities 3km/h to 25km/h, and terrestrial inclination magnitudes from -10.000° to 10.000°, which is key contribution rendered by this work. This work bridges geophysics, simulation, automation, and state agencies for the safety practices and measures for populous in any region of the world.**

Keywords— disaster management, automation, geo-seismic realization, motion control, geo-mechanics, earthquake, programmable, simulation, calibration, machine learning.

I. Introduction

The natural disasters occur on the globe every year with earthquake and floods being most devastating and horrible on the loss and damage benchmarks. The number of people reported affected by natural disasters (564.4million) was the highest since 2006 as compared to last 10 years [1], amounting to 1.5 times its annual average (224 million). The estimates of natural disaster economic damages (US$ 154 billion) place last year as the fifth costliest since 2006, 12% above the 2006-2015 annual average registered in CRED database. Earthquake or seismic events have proven to be the most obvious and recurring in all [2-3] natural disasters i.e. 14,568 in 2018. The top of the chart was in Indonesia on September 28, 2018, with 2,256 death tolls.

The only option to take preventive measures and implement pre-event and early warning mechanisms is the geo-seismic simulation systems. The trust-worthy simulation requires detailed geo-seismic and geo-mechanics coordination to realize the nearest natural occurrence of seismic events. The top 10 existing geo-seismic systems mentioned in research literature were studies in details and one common gap was observed exhibited in table I.

TABLE I. A Review of Top 13 Seismic Simulators

	Geo-Mechanics Simulation Systems and Platforms	*Common Gap*
1.	E-Defense Shake Table [4], Japan	Multi-parametric Geo-Seismic and Geo-Mechanics Realization/ Collaboration Engine
2.	Expanded Nevada [5] earthquake laboratory, USA	Multi-parametric Geo-Seismic and Geo-Mechanics Realization/ Collaboration Engine
3.	Ground Motion Simulator (GMS) [6], Turkey	Multi-parametric Geo-Seismic and Geo-Mechanics Realization/ Collaboration Engine
4.	myQuake [7], National Instruments	Multi-parametric Geo-Seismic and Geo-Mechanics Collaboration Engine
5.	The seismic events [8] variable rotation testbench	Multi-parametric Geo-Seismic and Geo-Mechanics Collaboration Engine
6.	GG SCHIERLE [9] shake table, California	Multi-parametric Geo-Seismic and Geo-Mechanics Realization/ Collaboration Engine
7.	The State Key Laboratory [10] for Disaster Reduction, China	Multi-parametric Geo-Seismic and Geo-Mechanics Realization/ Collaboration Engine
8.	UC Berkley Shake [11] Table, USA	Multi-parametric Geo-Seismic and Geo-Mechanics Realization/ Collaboration Engine
9.	San Diego's outdoor [12] shake table, Scripps Ranch, USA	Multi-parametric Geo-Seismic and Geo-Mechanics Realization/ Collaboration Engine
10.	focusTerra museum [13] in Zurich, Switzerland	Multi-parametric Geo-Seismic Realization/ Collaboration Engine
11.	CPPS Centre Simulator [13] in Sitten, Switzerland	Multi-parametric Geo-Seismic and Geo-Mechanics

	Geo-Mechanics Simulation Systems and Platforms	*Common Gap*
		Realization/ Collaboration Engine
12.	Tokyo Earthquake Simulation [15] Center, Japan	Multi-parametric Geo-Seismic and Geo-Mechanics Realization/ Collaboration Engine
13.	Four Degrees of Freedom [16] GMSP, Qatar	Multi-parametric Geo-Seismic and Geo-Mechanics Realization/ Collaboration Engine

Domain realization and perception assistance is the foremost constraint [4-18] in all simulation platforms design and implementations. In the geo-seismic domain, a plethora of contributions was observed in the simulation area from the theoretical and mathematical modeling aspect. The Tullis group simulator RSQSim [19] was appreciable for fault-friction modeling, fully dynamic single-event simulations, rate- and state state-dependent friction (RSF) modeling with a gap of wave modeling and ground motions realization. The ALLCAL [20] was one of the earthquake simulators developed by scientists of the Southern California Earthquake Center (SCEC) and belonged to the Tullis group of simulators. The ALLCAL used the Triangulation rule for the geometrical modeling and estimation of stresses and displacement to approximate fault friction and elastodynamics at a very abstract level had a gap of mechanical implementation and core geo-seismic realization. The Viscoelastic earthquake simulator for San Francisco Bay region [21] was a very noticeable approach towards seismicity functions with a gap of real surface motion kinematics, i.e. seismic waves and arrival times. The Virtual Quake (VQ) earthquake simulator [22] was a simulation-based forecast of the El Mayor-Cucapah region and evidence of predictability in simulated earthquake sequences was a successor of Virtual California (VC) can be used for forecasting and training mechanics. The gap in physical design and implementation [23] was very prominent in VQ contribution. The physics-based earthquake simulator replicated seismic hazard statistics across California [24] and compared its results with UCERF3 (Uniform California Earthquake Rupture Forecast, version 3 and RSQSim were reliant on parameterized [25, 26] ground-motion models (GMMs). The current state earthquake simulation [27] contribution also had gaps in geo-seismic realization [28-34] and its relationship with geo-mechanics implementation. The gaps in geo-seismic realization as a mechanical platform for physical implementation were observed in all [4-31] contributions had a common gap of geo-seismic realization.

II. Multi-parametric Geo-Seismic Realization Engine(GRE) Design and Implementation

The majority of ground motion simulation works either focused on the generation of seismic motions based on prolonged calibration or shake tables for active structural health assessment. In both cases, the uncertainty was expected for selected and in practice actuators types. The second major issue was the optimized multi-parametric domain modeling for precise coordination of physically robust ground mechanics. The section streamlined the geo-seismic realization engine that governed the optimized actuator dynamics to achieve the best of both worlds.

The objective of GRE was to convert seismological variables and parameters into actuator commands and sense them to ensure the accuracy of the simulation system. In seismology, there are two basic types of waves i.e. body waves and surface waves with sub-types of each. Body waves have two sub-types i.e. primary (P), secondary (S) and surface waves have Rayleigh (R) and Love (L) waves. The set of same type seismic waves has been termed as event and events clusters while the recurring sets are denoted as a pattern. For a sensing system, seismic waves are very specific ground motion events that need to be sensed in x, y, and z directions as D_X, D_Y, and D_Z. In figure 1, it can be observed that seismic waves study is focused on ground motion and anomalies in the lithosphere and crust only. The point where the seismic fault occurs and generates the earthquake is called hypocenter (C_H). The perpendicular point of (C_H) on earth surface is called epicenter (C_E). Both C_H and C_E have with seismic fault source location as F_L (x, y, z). The fault location for the collaborative localization method [30] using analytical and iterative solutions(CLMAI) is further specified as $CLMAI_F$ (F_{L1}, F_{L2}, F_{L3}, $GRE_{P\text{-}FL}$, t_{FL}) for GRE parameter P, at time t_{FL} for three geospatial fault sources or hypocenters. The point where seismic variables are observed is called a seismic station (S_S) with GPS coordinates S_S (x, y, z). The S_S can be further specified as $CLMAI_S$ for three seismic centers $CLMAI_S$ (S_{S1}, S_{S2}, S_{S3}, $GRE_{P\text{-}SS}$, t_{SS}) for GRE parameter P at t_{SS} as $GRE_{P\text{-}SS}$. The expected GRE parameter to be generated by fault location F_L (x, y, z) has noise discrimination [31] factor D_{SS} with percentage D_{SS} (%) when observed at S_S (x, y, z).

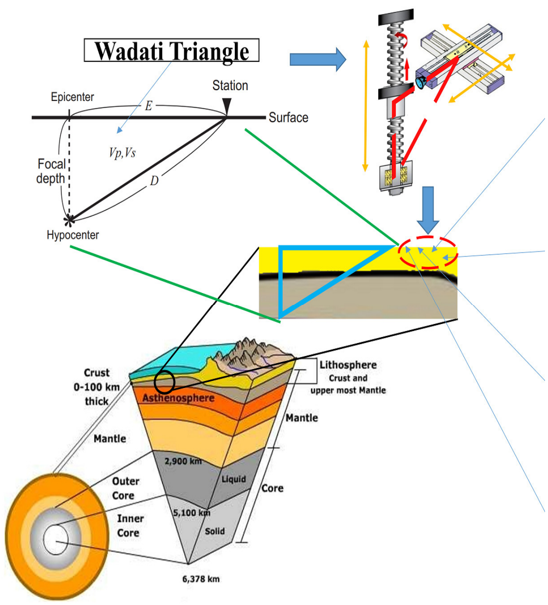

Fig. 1. Wadati Triangulation Mechanism

The entire refractive seismology from the pseudo-random occurrence of seismic fault to precision of observation at seismic stations is dependent on Pythagoras theorems and Wadati triangulation. The most basic segment in geomechanics modeling is ON/OFF, basic arithmetic, trigonometry and logarithmic operations for acceleration conversions to different intensity perception scales.

TABLE II. REALIZATION GEO-SEISMIC EVENTS AS MOTION CONTROL COMMANDS

	Geo-Seismic Domain	***GMSP Motion Control Domain***
Event Patterns	P-Waves Pattern(P_{EVENT})	M_{HS1} (CW + A-CW)
	S-Waves Pattern(S_{EVENT})	M_{VS1} (CW + A-CW)
	R-Waves Pattern(R_{EVENT})	M_{VS1} (CW) + M_{HS1} (CW) and M_{VS1} (A-CW) + M_{HS1} (A-CW)
	L-Waves Pattern(L_{EVENT})	M_{HS1} (CW) + M_{HS2} (CW) + M_{HS1} (A-CW) + M_{HS2} (A-CW)
	Earthquake Pattern(E_{EVENT})	$T_{PRE} + P_{EVENT} + T_{POST\text{-}P} + S_{EVENT} + T_{POST\text{-}S} + R_{EVENT}$ Or $T_{PRE} + P_{EVENT} + T_{POST\text{-}P} + S_{EVENT} + T_{POST\text{-}S} + L_{EVENT}$
Quantity of Patterns	Number of Waves(N_{WAVES})	n * $W_{EVENT}(P_{EVENT}, S_{EVENT}, R_{EVENT}, L_{EVENT})$
	Number of Earthquakes(E_{EQKS})	n * E_{EQKS}
Timers of Patterns	Arrival Time of P-Wave(T_{AP})	T_{PRE}
	Arrival Time of S-Wave(T_{AS})	$T_{AP} + T_{WP\text{-}P} + T_{POST\text{-}P}$
	Arrival Time of Rayleigh Wave(T_{AR})	$T_{AS} + T_{WP\text{-}S} + T_{POST\text{-}S}$
	Arrival Time of Love Wave(T_{AL})	$T_{AS} + T_{WP\text{-}S} + T_{POST\text{-}S}$
	Delay(T_{POST})	Post-Delay in Motors Commands
	Duration of Waves Pattern(T_{WP})	N_{WAVES} * T_W
	Duration of Earthquake(T_{EQK})	$T_{PRE} + T_{WP\text{-}P} + T_{POST\text{-}P} + T_{WP\text{-}S} + T_{POST\text{-}S} + T_{WP\text{-}R}$ Or $T_{PRE} + T_{WP\text{-}P} + T_{POST\text{-}P} + T_{WP\text{-}S} + T_{POST\text{-}S} + T_{WP\text{-}L}$
Magnitude of Pattern	Peak to Peak Amplitude of Waves(A_W) wave event X_{EVENT}	2 * $\sum_{i=0}^{n} X_{EVENT}$
	Magnitude of Earthquake ($M_{R\text{-}EQKS}$)	$\log(A_W/T_{EQK})$ or
Duration of a Single Wave	Time period of Waves(T_W)	Steps Timer for movement (CW + A-CW)
Frequency of a Single Wave Pattern	Frequency of a Wave(F_W)	$1 / T_W$
Distance Travelled	Distance Traveled by Waves(D_W)	Total Steps * T_W
	Distance Traveled by Unit Earthquake(D_{EQKS})	$D_{W\text{-}P} + D_{W\text{-}S} + D_{W\text{-}R}$ or $D_{W\text{-}P} + D_{W\text{-}S} + D_{W\text{-}L}$
Velocity of Waves (can be X and Y)	Velocity of P-Waves(V_P)	$D_{W\text{-}P} / T_{W\text{-}P}$
	Velocity of S-Waves(V_S)	$D_{W\text{-}S} / T_{W\text{-}S}$
	Velocity of R-Waves(V_R)	$D_{W\text{-}R} / T_{W\text{-}R}$
	Velocity of L-Waves(V_L)	$D_{W\text{-}L} / T_{W\text{-}L}$
Impact of P-Waves w.r.t to Equator and Poles	Angle of Incidence P-Waves(Θ_P) (can be X and Y)	(Not a Motor Commands as it is an Observation) Average Angle of P-Cluster where angle and acceleration is similar
Impact of S-Waves w.r.t to Equator and Poles	Angle of Incidence P-Waves(Θ_S) (can be X and Y)	(Not a Motor Commands as it is an Observation) Average Angle of S-Cluster where angle and acceleration is similar
Hypocentral Distance	Hypotenuse of Wadati Triangle (H_{WT})	B_{WT} / {cos((Θ_S+ Θ_P)/2)}
Epicentral Distance	Base of Wadati Triangle (B_{WT})	(T_{AS} - T_{AP}) * {(V_P* V_S)/ (V_P - V_S)}
Epi-Hypo Distance	Perpendicular of Wadati Triangle (P_{WT})	B_{WT} / {sin((Θ_S+ Θ_P)/2)}
Location of S_S	GPS Coordinates (Y°N, X°E)	No Motor Commands (Longitude and Latitude Values)

Table II exhibits 30 geo-seismic parameters that correspond to 30 unique motor commands to produce equivalent geo-mechanics. Let the five motors be first horizontal shaft motor be M_{HS1}, second horizontal shaft motor be M_{HS2}, first vertical shaft motor be M_{VS1}, second vertical shaft motor be M_{VS2}, and third vertical shaft motor be M_{HV3}. The terms "Steps" are dedicated to the unit movement of stepper motors. The "Timer" refers to the unit time between two consecutive steps.

In table II, the hypocenter and epicenter measurement assist in the computation of magnitude (M) and energy (E) of earthquakes. After seismic motion generation, the triangulation method is used to find the epicenter as the first step. Three seismic stations are a mandatory requirement for the triangulation method. The P, S, R and L waves can be sensed any high-sampling and precision bi-axial motion sensors. The wave velocity or motion needs accelerometers and angular displacement needs inclinometers tactically oriented in x, y and z-axis. The conversion of seismic variables into motion control commands in given below in Table II. Both steps and timers are dedicated to enabling or actuator control systems used for geo-seismic motion. In table II, all the information regarding GRE is given. Clockwise and anti-clockwise rotation is expressed as CW and A-CW. Those sensor values, which are used only for computation and not used for motor commands, have been termed as "Not a Motor Commands as it is an Observation" in table II. Further details can be read from references cited in the introduction.

The credibility or truthfulness of seismic events was authorized from at least 3 sources of observatories, i.e. seismic centers were three unique geospatial locations. There three different arrival times, as well as seismic noise induced in the signals, had to be differentiated from original or useful signals. The CLMAI and discriminant factor D was introduced to handle these criticalities narrated in table III.

TABLE III. REALIZATION GEO-SEISMIC EVENTS AS MOTION CONTROL COMMANDS

$CLMAI_S$ vector for three seismic centers	Time Vector of GPS Coordinates for GRE parameter under observation at a given time (S_{S1}, S_{S2}, S_{S3}, $GRE_{P\text{-}SS}$, t_{SS})	$CLMAI_S(S_{S1}(x_1, y_1, z_1), S_{S2}(x_2, y_2, z_2), S_{S3}(x_3, y_3, z_3), GRE_{P\text{-}SS}, t_{SS})$
Location of (C_H, C_E)	GPS Coordinates of Offset = (B_{WT}) from S_S ((Y°N, X°E)	S_S (Y°N, X°E) + (B_{WT} [sin{($\Theta_S + \Theta_P$)/2}]°N, B_{WT} [cos{($\Theta_S + \Theta_P$)/2}]°E)
$CLMAI_{FL}$ vector for three fault locations	Vector of GPS Coordinates with 3D offsets of (B_{WT}) from $CLMAI_S(S_{S1}, S_{S2}, S_{S3}, GRE_{P\text{-}FL}, t_{FL})$	$CLMAI_S(S_{S1}, S_{S2}, S_{S3}, GRE_{P\text{-}SS}, t_{SS})$ + {($B_{WT\text{-}SS1}$ [sin{($\Theta_{S\text{-}S1} + \Theta_{P\text{-}S1}$)/2}]°$N_1$, $B_{WT\text{-}SS1}$ [cos{($\Theta_{S\text{-}S1} + \Theta_{P\text{-}S1}$)/2}]°$E_1$, -$P_{WT\text{-}S1}$), {($B_{WT\text{-}SS2}$ [sin{($\Theta_{S\text{-}S2} + \Theta_{P\text{-}S2}$)/2}]°$N_2$, $B_{WT\text{-}SS2}$ [cos{($\Theta_{S\text{-}S2} + \Theta_{P\text{-}S2}$)/2}]°$E_2$, -$P_{WT\text{-}S2}$), {($B_{WT\text{-}SS3}$ [sin{($\Theta_{S\text{-}S3} + \Theta_{P\text{-}S3}$)/2}]°$N_3$, $B_{WT\text{-}SS3}$ [cos{($\Theta_{S\text{-}S3} + \Theta_{P\text{-}S3}$)/2}]°$E_1$, -$P_{WT\text{-}S3}$), $GRE_{P\text{-}SS}$, t_{SS}}
Noise Discrimination Factor Dss(%)	The magnitude of the percentage difference between $CLMAI_{SS}$ and $CLMAI_{FL}$	(Not a Motor Commands as it is an Observation) {(|$CLMAI_{FL}$ - $CLMAI_{SS}$|)/ $CLMAI_{FL}$} x 100

III. IMPLEMENTATION OF GRE ON A PROGRAMMABLE GEO-MECHANICS GROUND MOTION SIMULATOR

An open-source programmable mechatronics ground motion was needed to test the conceptual framework devised in section II. The work [16] was chosen as a testing ground for GRE exhibited in figure 2.

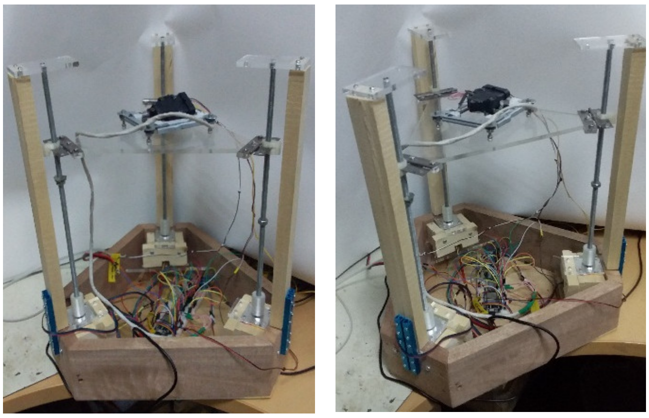

Fig 2. GMSP [16] Assembled Photographs

The GMSP consisted of a motion control system and a motion-sensing system. In GMSP, the GRE was used to produce the ground mechanics through a four degree of a motion system with 4 stepper motors. The a biaxial bi-sensor node as given in works [17 – 21] was capitalized to sense the high-frequency motions.

IV. RESULTS AND DISCUSSION

The GRE was programmed in the GSMP SoC module to perform the core experiments. The experiments were dual verified by sensing through PC based oscilloscope interfaced with Matlab. The GRE was tested for following geo-mechanics automation using setup shown in figure 3:

1. Three types of Seismic Waves, P, S & R.
2. A Characteristic Earthquake Sequence.

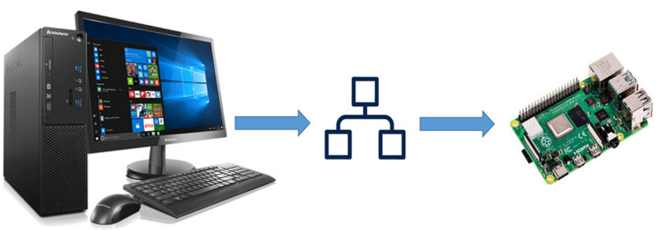

Fig 3. Data Acquisition System for GRE Verification

The results were observed from two sources, i.e. the Tektronix oscilloscope and MATLAB serial input. The GMSP results are very fertile and perceivable by seismologists and geologists.

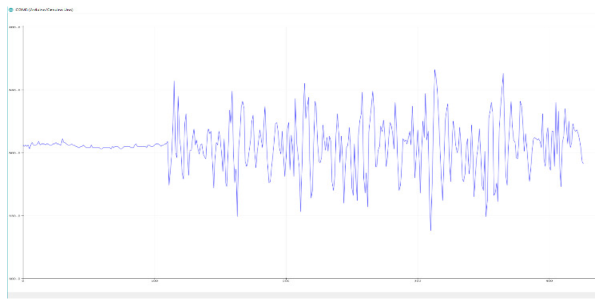

Fig 4. P-Waves observed in MATLAB for 8Hz on the x-axis [16] (without GRE)

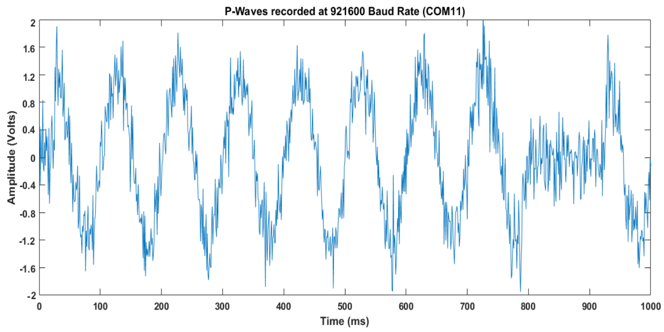

Fig 5. P-Waves observed in MATLAB for 8Hz on the x-axis with GRE

The impact of GRE motor control commands and multi-parametric control actuation variables are eloquent in figure 5 for 8Hz uniform P-waves without seismic parameter damping.

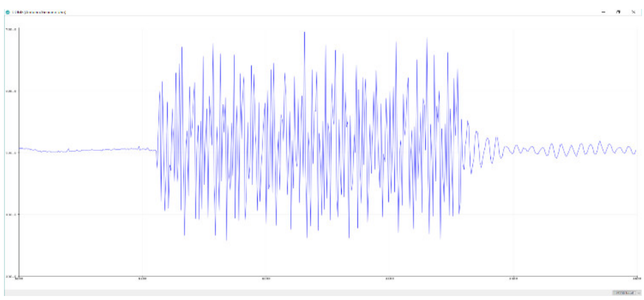

Fig 6. S-Waves observed in MATLAB for 4Hz on the y-axis (without GRE)

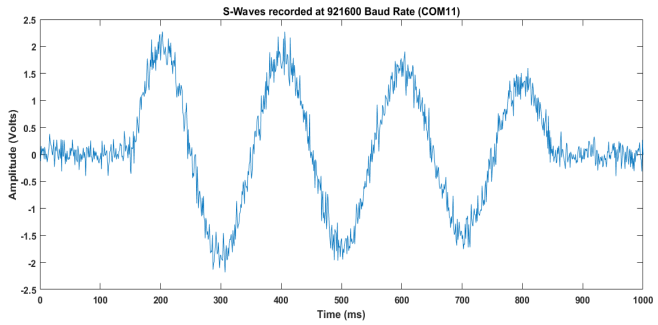

Fig 7. S-Waves observed in MATLAB for 4Hz on the y-axis (with GRE)

The results captured in MATLAB were very self-explanatory. An obvious difference in terms of waves nature and captured sensor values are visible in figures 6 and 7.

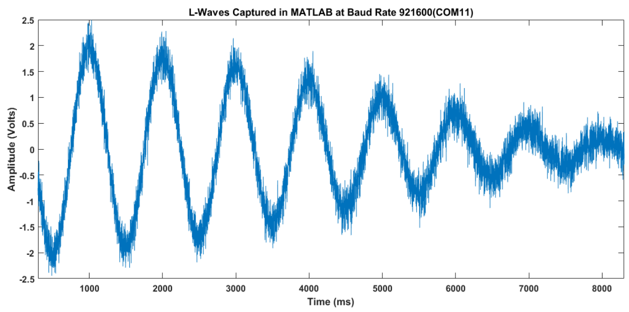

Fig 8. R-Waves observed in MATLAB for 8Hz on the y-axis (with GRE)

The contribution of GRE is presented in figure 8 as one of the key contributions in accurate geo-mechanics. Furthermore, a characteristic earthquake pattern 8 P-waves, 4 S-waves, 3 R-waves and 3 L-waves with a duration of 4 seconds. The GRE was able to deliver very swift and sharp results on the GMSP and assured its reliability and capabilities for a much challenging simulation.

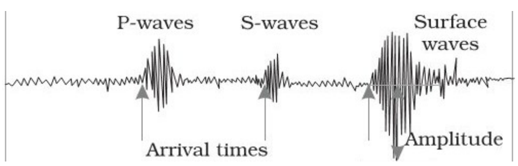

a. Standard Earthquake Pattern

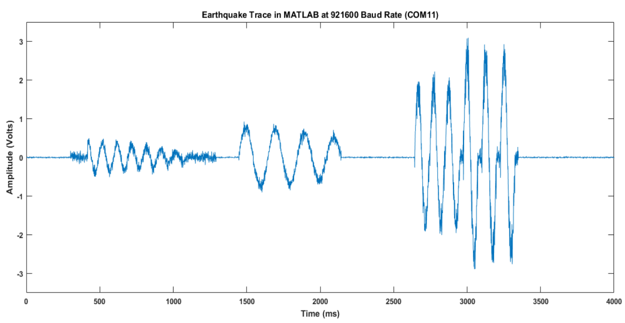

b. GMSP Generated Pattern for Characteristic Valdivia Incident

Fig 9. Valdivia Earthquake Simulation on GMSP

The GMSP generated earthquake from the data collected from the IRIS database and converted into motor controls and programmed into the system as shown in the fig 9.

Furthermore, the serial input of ESP32 was connected to PC to observe long-term results in MATLAB and plotted as real-time time-series for further analysis. The results are very ideal for seismological studies and future observations of other earthquakes occurred over the course of time.

V. Conclusion

A multi-parametric geo-seismic realization with detailed parametric study and derivation of motor commands added significant value to capabilities of the current state of the art geo-seismic simulator. A 4 degree-of-freedom seismic wave ground motions simulation platform for P, S and Rayleigh waves developed in our previous works was tested and demonstrated promising results. The 22 multi-variable parameters equated with motor commands served a real-life value addition to seismic simulators to have much detailed scientific applications. This constitutes a strong tool to train algorithms for machine learning and AI as well as deep learning models.

Acknowledgment

This publication was made possible by NPRP grant # 8-1781-2-725 and NPRP grant # 10-0102-170094 from the Qatar National Research Fund (a member of Qatar Foundation). The statements made herein are solely the responsibility of the authors.

References

[1] D. Guha-Sapir, P. Hoyois, P. Wallemacq and R. Below, “Annual Disaster Statistical Review 2016 The numbers and trends,” Centre for Research on the Epidemiology of Disasters (CRED), 2016.

[2] S. Kimball, Earthquake Statistics. United States Geological Survey. Retrieved May 10, 2017.

[3] Geophysical Journal International, Volume 179, Issue 3, Pages 1669–1678, https://doi.org/10.1111/j.1365-246X.2009.04363.xM, 2009.

[4] U. E. Dorka, F. O. Santacana, and T. A. Khan, “E-DEFENSE, JAPAN - WORLD'S LARGEST SHAKING TABLE,” *NEES Consortium*, 2009.

[5] Expanded Nevada Earthquake Laboratory, USA, Accessed on: November 3, 2019. [Online] Available: http://www.seismo.unr.edu/

[6] A. Aytun, “A NEW 3-D EARTHQUAKE SIMULATOR FOR TRAINING AND RESEARCH PURPOSES,” in 13th *World Conference on Earthquake Engineering*, Vancouver, B.C., Canada, Paper No. 3429, 2010.

[7] K. Othani, T. Hayama, N. Ogawa, M. Sato, PROJECT ON 3-D FULL-SCALE EARTHQUAKE TESTING FACILITY, THE FOURTH REPORT, 2006.

[8] K. Yao, W. Huang, C. Lin, P. Wu, J. Chiang, “Virtual Instrumentation Design on Earthquake Simulation System,” *International Conference on Artificial Intelligence and Industrial Engineering*, 2015.

[9] A. Velikoseltsev, A. Yankovsky, V. Khvostov, “Implementation of the high accuracy variable rotation testbench: seismology options,” in *4th IWGoRS workshop Tutzing*, 2016.

[10] A.N Swaminathen, P.Sankari, “Experimental Analysis of Earthquake Shake Table,” *American Journal of Engineering Research*, e-ISSN: 2320-0847 p-ISSN : 2320-0936, Volume-6, Issue-1, pp-148-151, 2017.

[11] W. Shi, “SHAKING TABLE EXPERIMENTAL STUDY OF REINFORCED CONCRETE HIGH-RISE BUILDING,” in *Twelfth World Confernce in Earthquake Engieering*, 2012.

[12] J. E. Barnes, “Seismic Modeling with an Earthquake Shake Table,” *DigitalCommons*, 2012.

[13] S. Pei, "FULL-SCALE SHAKE TABLE TESTING OF A TWOSTORY MASS TIMBER BUILDING WITH RESILIENT ROCKING WALL LATERAL SYSTEM", November 2017.

[14] A. Ebeido et al, "Large Scale Geotechnical Shake Table Testing at the University of California San Diego," in *2nd GeoMEast International Congress and Exhibition on Sustainable Civil Infrastructures*, 2018.

[15] F. Vieux-Champagne et al , "Experimental Analysis of a Shake Table Test of Timber-Framed Structures with Stone and Earth Infill," in *Earthquake Spectra, Volume 33, No. 3, pages 1075–1100*, 2017.

[16] F. Touati, H. Tariq, D. Crescini, A. B. Manouer, "Design and Simulation of a Green Bi-Variable Mono-Parametric SHM Node and Early Seismic Warning Algorithm for Wave Identification and Scattering," in *14th International Wireless Communications & Mobile Computing Conference*, 2018.

[17] F. Touati, H. Tariq, A. B. Mnaouer and D. Crescini, "IoT and IoE prototype for scalable infrastructures, architectures and platforms," *International Symposium on Ubiquitous Networking*, pp 202-216, 2018.

[18] H. Tariq, A. Tahir, F. Touati, M. Al-Hitmi, A. B. Mnaouer, and D. Crescini, "Geographical Area Network—Structural Health Monitoring Utility Computing Model," *International Journal of Geo-Information*, 2019.

[19] R. D. Keith, and H. D. James, "RSQSim Earthquake Simulator," *Seismological Research Letters*, 2012.

[20] N. W. Steven, "ALLCAL Earthquake Simulator," *Seismological Research Letters,* 2012.

[21] F. Fred, "A Viscoelastic Earthquake Simulator with Application to the San Francisco Bay Region," *Bulletin of the Seismological Society of America,* 2009.

[22] R. Y. Mark et al, "The Virtual Quake earthquake simulator: a simulation-based forecast of the El Mayor-Cucapah region and evidence of predictability in simulated earthquake sequences Earthquake Simulator," *Geophysical Journal International,* 2015.

[23] H. Shunsuke, "A physics-based Monte Carlo earthquake disaster simulation accounting for uncertainty in building structure parameters," *Fourteenth International Conference on Computational Science*, 2014.

[24] Muneo, H.; and Tsuyoshi, I. Current state of integrated earthquake simulation for earthquake hazard and disaster. *Journal of Seismology*, 2007.

[25] H. Tariq, A. Tahir, F. Touati, M. Al-Hitmi, A. B. Mnaouer, and D. Crescini, "Structural Health Monitoring and Installation Scheme deployment using Utility Computing Model," *European Conference on Electrical Engineering and Computer Science*, 2018.

[26] H. Tariq, F. Touati, M. Al-Hitmi, A. B. Mnaouer, A. Tahir and D. Crescini, "IoT and IoE prototype for scalable infrastructures, architectures and platforms," *International Robotics & Automation Journal*. 4. 10.15406/iratj.2018.04.00144, 2019.

[27] M.A. Shah, T. Khan and M.K. Abbasi, "Communications, Applications, Technology and Beyond: A Survey on Smart Grid," *Sindh Univ. Res. Jour. (Sci. Ser.) Vol. 48 (3) 651-656*, 2016.

[28] H. Tariq, F. Touati, M. Al-Hitmi, A. B. Mnaouer, and D. Crescini, et al, "Design and Implementation of Information Centered Protocol for Long Haul SHM Monitoring," in *International Wireless Communications and Mobile Computing Conference*, 2019.

[29] A. Galli, F. Touati, M. Al-Hitmi, A. B. Mnaouer, and D. Crescini, "Environmentally Powered Multiparametric Wireless Sensor Node for Air Quality Diagnostic," *Sensors and Materials* 27(2):177-189, January 2015.

[30] U. Asghar et al, "Development of Highly Efficient Multi-Invariable Wireless Sensor System Design for Energy Harvesting," *arXiv:1802.05755*, 2018.

[31] Engineering, Equipment and Machinery. [online] Allied Market Research, p.201. https://www.alliedmarketresearch.com/structural-health-monitoring-market, [Accessed 13 Oct. 2018].

[32] Chang, F. Structural health monitoring. *Lancaster, Pa: DEStech Publ*, 2013.

[33] F. Touati, H. Tariq, M. Al-Hitmi, A. B. Mnaouer, and D. Crescini, IoT and IoE prototype for scalable infrastructures, architectures and platforms. *4th International Symposium, UNet 2018, Hammamet, Tunisia, DOI: 10.1007/978-3-030-02849-7_18*, 2018.

[34] H. Tariq, F. Touati, M. Al-Hitmi, A. B. Mnaouer, and D. Crescini, A Real-time Early Warning Seismic Event Detection Algorithm using Smart Geo-Spatial Bi-axial Inclinometer Nodes for Industry 4.0 Applications, *Applied Sciences*, 2019.